Gauge-Invariant Dressed Thermodynamics of Ultrastrong-Coupling Mito-Polaritons: Virtual-Photon Passivity, Positive Zero-Point Energy Shifts, and Dipole-vs-Coulomb Dark-Mode Invariance

Lluis Eriksson
Independent Researcher (https://github.com/lluiseriksson)
Dressed-USC Audit Continuing ARR-2025-2AQXS44H6Z8GQAG2 and ARR-2026-1E91AXEJYT890TQC

November 27, 2026

Abstract

In ARR-2026-1E91AXEJYT890TQC (Nov. 26, 2026), we showed that the 71.0-THz mitochondrial cristae polariton model of Yang, Gu, and Song (bioRxiv:10.64898/2026.09.10.750628v1, Sep. 2026, unrefereed) operates at resonance ($\omega_c = \omega_0 = 87$ THz) in the ultrastrong-coupling (USC) regime ($\eta = g/\omega_0 = 1264/6177 \approx 0.2046 > 0.1$) with a +3.61 THz Hopfield A^2 shift ($\nu_+^{\mathrm{Hop}} = 7569/71 \approx 106.61$ THz). In USC, bare-basis open-system equations break gauge invariance and predict unphysical vacuum heating or perpetual work extraction from virtual excitations. Here we derive the exact gauge-invariant dressed quantum thermodynamics of USC mito-polaritons, backed by a zero-floating-point verification suite (MITO-USC-DRESSED-THERMO-CERT-1.0) with 18 constructive Lean 4.36.0 integer/rational theorems (0 sorry, 0 custom axioms, 0 Classical.choice, -DwarningAsError=true), 16 canonical exact-$\mathbb{Q}$ certificates (C01--C16), and 26 unit/forgery/AST tests: (i) for every detuning (ω_c, ω_0, g), the Hopfield A^2 normal frequencies obey $(\nu_+ + \nu_-)^2 = (\omega_c + \omega_0)^2 + 4g^2$, enforcing a strictly positive zero-point energy (ZPE) shift; at resonant 71/87 THz, $\Delta E_{\mathrm{ZPE}} = \frac{128}{71}\, h \cdot \mathrm{THz} \approx 7.456$ meV $\approx 0.279\, k_B T$ per coupled mode, reaching the order-of-magnitude Helfrich bilayer bending rigidity scale ($\kappa_{\mathrm{bend}} \approx 15\, k_B T$) at $M = 54$ coupled modes (before geometric curvature factors); (ii) exact resonant 4×4 symplectic diagonalization yields identical ground-state bare photon and CH_2 phonon occupations in both Coulomb ($p \cdot A$) and Dipole (PZW, $d \cdot E$) gauges, $n_{\mathrm{virt}} = (\omega_0 - \nu_-)^2/(4\omega_0\nu_-) = 64/6177 \approx 0.01036$, exceeding bare 87-THz thermal occupation ($\bar{n}_{\mathrm{th}}(\omega_0) < 2 \times 10^{-6}$ at 310 K) by $> 5180\times$, with exact position squeezing 6177/6305, marginal vacuum entanglement $\det(2V_a) = 1 + 4g^2/(\nu_+ + \nu_-)^2 > 1$, and exact interaction–diamagnetic cancellation $\langle G|H_{\mathrm{int}} + H_{A^2}|G\rangle = 0$; (iii) by exact thermodynamic passivity ($\mathcal{W}_{\mathrm{erg}}(|G\rangle, H_C) = 0$) and dressed energy pinching ($C_{\Delta_D}(|G\rangle) = 0$), virtual photons cannot drive ATP synthesis or incur holding power, whereas naive bare-basis master equations predict spurious excitation exceeding the true dressed lower-polariton KMS upward rate $\gamma_\uparrow(\nu_-) = e^{-\beta h\nu_-}\gamma_\downarrow$ at 310 K by $> 610\times$ ($\approx 615\times$ at 71 THz, $\approx 477\times$ at 79 THz, $\approx 502\times$ at 65 THz); (iv) under PZW transformation, canonical matter weights swap ($w_{\mathrm{mat}}^{\mathrm{Coul}} = 7569/12610 \leftrightarrow w_{\mathrm{mat}}^{\mathrm{Dip}} = 5041/12610$), while the physical single-branch dipole transition element $|\langle G|\sqrt{2\omega_0}q_b|\mathrm{MP}^-\rangle|^2 = \omega_0\nu_-/(\omega_0^2 + \nu_-^2) = 6177/12610 \approx 0.4899$ (half the two-branch quadrature sum 6177/6305) and the $(N-1)$-dimensional dark manifold remain strictly gauge-invariant; and (v) single-mode $\Delta E_{\mathrm{ZPE}} \approx 7.456$ meV exceeds the 2.546 meV ($k_B T \ln 1.1$) barrier shift for +10% enzymatic turnover by $> 2.9\times$ as a collective energetic ceiling, while $1/N$ dilution across $N = 10^6$–10^8 uncorrelated dipoles restricts passive Regime I catalysis to coherent collective reaction-coordinate coupling or localized few-dipole microdomains.

1 Introduction and Epistemic Scope

In ARR-2025-2AQXS44H6Z8GQAG2 [3], we formulated an operational resource-boundary pipeline bounding the continuous power required to sustain quantum coherence across biological membranes. Applying that framework in ARR-2026-1E91AXEJYT890TQC [4] to the unrefereed September 2026 preprint of Yang, Gu, and Song [9] revealed that resonant $\nu_- = 71$ THz and $\omega_0 = 87$ THz place the proposed cristae polariton squarely in the ultrastrong-coupling (USC) regime ($\eta = 1264/6177 \approx 0.2046$) [7].

In USC, standard bare-basis approximations fail catastrophically [2, 8]: the true ground state $|G\rangle$ is a two-mode squeezed vacuum populated with virtual bare photons and phonons, so naive bare-basis master equations predict spurious zero-temperature heating and perpetual work extraction. Throughout, we use ordinary frequencies $\omega_c, \omega_0, \nu_\pm$ in THz (with quantum energy $h\nu$, setting $h = 1$ in dimensionless canonical coordinates). As in [4], we neither endorse nor refute the unrefereed empirical claims of [9], but derive exact thermodynamic constraints governing any USC vibrational polariton at 310 K.

2 Five Exact Dressed-USC Results

2.1 Universal Positive ZPE Shift and Helfrich Scale Benchmark

The gauge-invariant Hopfield A^2 Hamiltonian [6] in dimensionless canonical coordinates (q_a, p_a, q_b, p_b) takes the minimal-coupling Coulomb form

$$H_C = \frac{1}{2}p_a^2 + \frac{1}{2}(p_b + 2gq_a)^2 + \frac{1}{2}\omega_c^2 q_a^2 + \frac{1}{2}\omega_0^2 q_b^2. \quad (1)$$

Its normal frequencies satisfy $\nu_+^2 + \nu_-^2 = \omega_c^2 + \omega_0^2 + 4g^2$ and $\nu_+\nu_- = \omega_c\omega_0$. Adding $2\nu_+\nu_-$ proves a detuning-universal identity (Lean Thms. 1–2):

$$(\nu_+ + \nu_-)^2 = (\omega_c + \omega_0)^2 + 4g^2 \implies \nu_+ + \nu_- > \omega_c + \omega_0. \quad (2)$$

Thus forming a Hopfield polariton *always* raises the ground-state zero-point energy $\Delta E_{\mathrm{ZPE}} = \frac{1}{2}h(\nu_+ + \nu_- - \omega_c - \omega_0) > 0$. At resonance ($\omega_c = \omega_0$, $\nu_+\nu_- = \omega_0^2$), clearing ν_- gives the exact square identity (Thm. 3; `C01`, Fig. 1a):

$$\nu_+ + \nu_- - 2\omega_0 = \frac{(\omega_0 - \nu_-)^2}{\nu_-} = \frac{256}{71}\ \mathrm{THz}, \quad (3)$$

yielding $\Delta E_{\mathrm{ZPE}} = \frac{128}{71}\,h \cdot \mathrm{THz} \approx 7.456$ meV $\approx 0.279\,k_BT$ per coupled mode at $T = 310$ K. Benchmarked against the bare Helfrich lipid bilayer bending modulus $\kappa_{\mathrm{bend}} \approx 15\,k_BT \approx 400.7$ meV [5], $M = 53$ modes remain below κ_{bend} (395.2 meV, `C02`) whereas $M \geq 54$ modes exceed it (402.6 meV, Thm. 4; `C03`, Fig. 1b). (Full mechanical deformation thresholds scale further by dimensionless curvature geometry, e.g. $8\pi\kappa_{\mathrm{bend}}$ for closed spherical folds, so $M = 54$ provides a conservative order-of-magnitude benchmark.)

2.2 Exact Virtual Occupation, Squeezing, Entanglement, and Cancellation

Setting $S := \nu_+ + \nu_-$, exact 4×4 symplectic diagonalization of (1) at resonance ($\omega_c = \omega_0$) gives ground-state covariances

$$\langle q_a^2\rangle_G = \langle q_b^2\rangle_G = \frac{1}{S}, \qquad \langle p_a^2\rangle_G = \langle p_b^2\rangle_G = \frac{\nu_+^2 + \nu_-^2}{2S}. \quad (4)$$

Substituting (4) into $n_a = \frac{1}{2}(\omega_0\langle q_a^2\rangle_G + \langle p_a^2\rangle_G/\omega_0 - 1)$ and using $2\omega_0^2 = 2\nu_+\nu_-$ collapses the numerator into $S(S - 2\omega_0)$ (Thm. 5):

$$n_{\mathrm{virt}} = \langle G|a^\dagger a|G\rangle = \langle G|b^\dagger b|G\rangle = \frac{(\omega_0 - \nu_-)^2}{4\omega_0\nu_-} = \frac{64}{6177} \approx 0.01036. \quad (5)$$

At 310 K, bare 87-THz thermal occupation obeys $\bar{n}_{\mathrm{th}}(\omega_0) < 2 \times 10^{-6}$ [4], so virtual bare excitations outnumber bare thermal quanta by $> 5180\times$ (Thm. 6; `C05--C08`, Fig. 2a). Simultaneously, bare coordinates undergo exact position squeezing $\langle q^2\rangle_G/\langle q^2\rangle_0 = 2\omega_0\nu_-/(\omega_0^2 + \nu_-^2) = 6177/6305 < 1$ (Thm. 7), while the marginal symplectic purity invariant satisfies (Thm. 8; Fig. 2b)

$$\det(2V_a) = \frac{2(\nu_+^2 + \nu_-^2)}{(\nu_+ + \nu_-)^2} = 1 + \frac{4g^2}{(\nu_+ + \nu_-)^2} > 1, \quad (6)$$

certifying strict light–matter entanglement in $|G\rangle$. Moreover, $\langle G|H_0|G\rangle = h\omega_0(1 + 2n_{\mathrm{virt}}) = \frac{1}{2}h(\nu_+ + \nu_-) = \langle G|H_C|G\rangle$, proving exact cancellation of attractive $p\cdot A$ and repulsive A^2 ground-state energies: $\langle G|H_{\mathrm{int}} + H_{A^2}|G\rangle = 0$ identically (Thms. 9, 17).

2.3 Thermodynamic Passivity and Dressed KMS vs. Spurious Bare Heating

Under the Power–Zienau–Woolley (PZW) unitary $U_{\mathrm{PZW}} = e^{-2ig q_a q_b}$, $H_D = U_{\mathrm{PZW}}^\dagger H_C U_{\mathrm{PZW}} = \frac{1}{2}(p_a - 2gq_b)^2 + \frac{1}{2}p_b^2 + \frac{1}{2}\omega_0^2(q_a^2 + q_b^2)$ preserves the spectrum, resonant covariances (4), and $n_{\mathrm{virt}} = 64/6177$ identically (Thm. 10). Because $|G\rangle$ is the unique lowest eigenstate of H_C, any unitary or passive evolution obeys $\mathrm{Tr}(H_C\rho) \geq E_0$, yielding identically zero ergotropy [1] $\mathcal{W}_{\mathrm{erg}}(|G\rangle, H_C) = 0$ (Thm. 11; `C09--C11`) and zero dressed energy-pinching coherence $C_{\Delta_D}(|G\rangle) = 0$ (Thm. 12). Hence virtual photons *cannot* power ATP synthesis or incur holding power.

Conversely, a naive bare-basis Lindblad dissipator $\gamma_0\mathcal{D}[a]$ applied to $|G\rangle$ excites polaritons at rate $\propto n_{\mathrm{virt}}\gamma_0 = (64/6177)\gamma_0$, violating the Second Law against the true dressed lower-polariton KMS upward rate [2] $\gamma_\uparrow(\nu_-) = e^{-\beta h\nu_-}\gamma_\downarrow$. Crucially, $\gamma_\uparrow$ is governed by the *dressed* frequency ν_- rather than bare $\omega_0 = 87$ THz: at 310 K ($k_BT = 26.713$ meV), $e^{-\beta h\nu_-} \approx 1.683 \times 10^{-5} < 1/59{,}000$ at 71 THz, $4.879 \times 10^{-6} < 1/204{,}000$ at 79 THz, and $4.262 \times 10^{-5} < 1/23{,}400$ at 65 THz. Thus under a flat-bath benchmark ($\gamma_0 = \gamma_\downarrow$, with branch splitting and spectral density ratios $J(\nu_-)/J(\omega_0)$ introducing $\mathcal{O}(1)$ prefactors), naive bare-basis heating still exceeds true dressed KMS excitation by $> 610\times$ ($\approx 615\times$) at 71 THz (`C14`), $> 470\times$ ($\approx 477\times$) at 79 THz (`C15`), and $> 500\times$ ($\approx 502\times$) at 65 THz (`C16`; Thm. 14, Fig. 3b)—exhibiting a non-monotonic competition between growing n_{virt} and growing thermal factor $e^{-\beta h\nu_-}$ as ν_- softens.

2.4 PZW Gauge Swap and Invariant Dark-Mode Scattering

In Coulomb gauge, the lower-polariton canonical matter weight is $w_{\mathrm{mat}}^{\mathrm{Coul}} = \omega_0^2/(\omega_0^2 + \nu_-^2) = 7569/12610 > 1/2$ [4]; under PZW transformation into Dipole gauge, canonical weights swap to $w_{\mathrm{mat}}^{\mathrm{Dip}} = \nu_-^2/(\omega_0^2 + \nu_-^2) = 5041/12610 < 1/2$ with exact complementarity $w_{\mathrm{mat}}^{\mathrm{Coul}} + w_{\mathrm{mat}}^{\mathrm{Dip}} = 1$ (Thm. 13; `C12--C13`, Fig. 3a). Crucially, for a physical vibrational bath coupled to the gauge-invariant dipole coordinate q_b, exact diagonalization gives the *single-branch* transition matrix element

$$|\langle G|\sqrt{2\omega_0}\,q_b|\mathrm{MP}^-\rangle|^2 = \frac{\omega_0\nu_-}{\omega_0^2 + \nu_-^2} = \frac{6177}{12610} \approx 0.48985, \quad (7)$$

correctly approaching $1/2$ as $g \to 0$ (whereas the two-branch sum $2\omega_0\langle G|q_b^2|G\rangle = 2\omega_0\nu_-/(\omega_0^2 + \nu_-^2) = 6177/6305$ approaches 1). Because U_{PZW} acts exclusively on the bright collective coordinate Q_B, the $(N-1)$-dimensional dark manifold remains strictly invariant with zero $1/N$ protection in every gauge (Thm. 15).

2.5 Collective Catalysis Ceiling and $1/N$ Dilution

Although virtual photons yield zero cyclic work ($\mathcal{W}_{\rm erg} = 0$), a +10% enzymatic turnover enhancement requires a barrier shift of $|\Delta E_a| = k_B T \ln(11/10) \approx 2.546$ meV at 310 K. Single-mode ZPE shifting ($\Delta E_{\rm ZPE} \approx 7.456$ meV) exceeds $|\Delta E_a|$ by $> 2.9\times$ (Thms. 16, 18; `C14`). However, across an ensemble of $N = 10^6$–10^8 uncorrelated lipid dipoles (Sec. 2.4), the per-molecule vacuum shift dilutes as $\mathcal{O}(\Delta E_{\rm ZPE}/N)$: thus 7.456 meV acts as a *collective single-mode ceiling*, and realizing a +10% catalytic shift requires either coherent reaction-coordinate coupling to the collective bright mode or localized few-dipole microdomains (plus resonant IR driving for irradiance-triggered gains over dark controls).

3 Formal Certification Scope and Reproducibility

Exact verification boundary. Layer 1 (`src/lean/MitoUscDressedThermoCert.lean`, 18 constructive integer/rational theorems compiled under Lean 4.36.0 `-DwarningAsError=true` without Mathlib, audited via `#print axioms` to depend strictly on `propext` and `Quot.sound`: `0 sorry`, `0` custom axioms, `0 Classical.choice`, Table 1) certifies the exact algebraic, sum-square, squeezing, entanglement-purity, finite-level passivity, PZW-swap, dressed-KMS, and catalytic-margin inequalities over $\mathbb{Z}$ and $\mathbb{N}$. Layer 2 (`src/python/mito_usc_dressed_thermo_verifier.py`, AST-audited zero-float) verifies all 16 canonical exact-$\mathbb{Q}$ certificates (`C01--C16`, Table 2, archived in `data/certificates/`) and passes all 26 unit/forgery tests under `pytest -q`. Infinite-dimensional Hilbert-space operator diagonalization, unitary PZW conjugation, bosonic ergotropy, and KMS master-equation derivations reside in Section 2 prose rather than inside the Lean kernel.

All Lean 4 proofs (`src/lean/`), zero-float verifier (`src/python/`), 16 JSON certificates (`data/certificates/`), and `MANIFEST.sha256` are archived directly in this public AIRR record under MIT (code/Lean/data) and CC-BY-4.0 (manuscript/figures).

AI Assistance Disclosure. Google Antigravity assisted with Lean 4 proof engineering, zero-float verifier implementation, figure/test automation, and LaTeX drafting. The author verified every derivation, Lean axiom audit, certificate check, and figure, and takes full responsibility for all contents.

References

[1] Armen E. Allahverdyan, Roger Balian, and Theo M. Nieuwenhuizen. Maximal work extraction from finite quantum systems. *Europhysics Letters*, 67(4):565–571, 2004.

[2] Félix Beaudoin, Jay M. Gambetta, and Alexandre Blais. Dissipation and ultrastrong coupling in circuit QED. *Physical Review A*, 84:043832, 2011.

[3] Lluis Eriksson. Geometry, membranes, and life as a resource boundary: A correct-by-construction operational pipeline from static suppression to maintenance costs. 2025. AIRR.SCIENCE record ARR-2025-2AQXS44H6Z8GQAG2 (ai.viXra:2512.0085, v1 Dec 2025; v2 Jul 2026).

[4] Lluis Eriksson. Mito-polaritons meet the resource boundary: Exact Hopfield A^2 invariants, thermodynamic maintenance horizons, and constructive Lean 4 certificates for the 71-THz mitochondrial quantum state. 2026. AIRR.SCIENCE record ARR-2026-1E91AXEJYT890TQC (accepted Nov 26, 2026).

[5] Wolfgang Helfrich. Elastic properties of lipid bilayers: Theory and possible experiments. *Zeitschrift für Naturforschung C*, 28:693–703, 1973.

[6] John J. Hopfield. Theory of the contribution of excitons to the complex dielectric constant of crystals. *Physical Review*, 112(5):1555–1567, 1958.

[7] Anton Frisk Kockum, Adam Miranowicz, Simone De Liberato, Salvatore Savasta, and Franco Nori. Ultrastrong coupling between light and matter. *Nature Reviews Physics*, 1:19–40, 2019.

[8] Omar Di Stefano, Alessio Settineri, Vincenzo Macrì, Luigi Garziano, Roberto Stassi, Salvatore Savasta, and Franco Nori. Resolution of gauge ambiguities in ultrastrong-coupling cavity quantum electrodynamics. *Nature Physics*, 15:803–808, 2019.

[9] Yu Yang, Zhenglong Gu, and Bo Song. A quantum state of mitochondria in the living cell. 2026. bioRxiv preprint 10.64898/2026.09.10.750628v1, 15 September 2026 (unrefereed).

Table 1: All 18 constructive Lean 4.36.0 theorems in `src/lean/MitoUscDressedThermoCert.lean` (`0 sorry`, `0 Classical.choice`, `-DwarningAsError=true`).

#	Lean Theorem Identifier	Exact Formalized Algebraic/Arithmetic Statement (over $\mathbb{Z}$ or $\mathbb{N}$)
1	`detuned_zpe_sum_square_identity`	$\nu_+^2+\nu_-^2=\omega_c^2+\omega_0^2+4g^2 \wedge \nu_+\nu_-=\omega_c\omega_0 \implies (\nu_++\nu_-)^2=(\omega_c+\omega_0)^2+4g^2$
2	`strict_positive_zpe_shift_all_detunings`	$S,U\geq 0 \wedge g>0 \wedge S^2=U^2+4g^2 \implies U<S$ (universal positive ZPE)
3	`resonant_zpe_exact_rational_shift`	$\nu_+\nu_-=\omega_0^2 \implies \nu_-(\nu_++\nu_--2\omega_0)=(\omega_0-\nu_-)^2\geq 0$; $\Delta E_{\rm ZPE}\in(7.45,7.46)$ meV
4	`helfrich_bending_mode_count_horizon`	$53\cdot 7456<400700<54\cdot 7456\leq M\cdot 7456$ ($M\geq 54$ crosses $15\,k_BT$ benchmark)
5	`exact_resonant_virtual_occupation_identity`	$Q+2\omega_0^2=S^2 \implies 2\omega_0^2+Q-2\omega_0 S=S(S-2\omega_0)$; $n_{\rm virt}=64/6177$
6	`virtual_exceeds_thermal_5000x`	$64/6177>1/100$; $64\cdot 500000>5180\cdot 6177$ ($>5180\times$ bare 87-THz thermal)
7	`ground_state_quadrature_squeezing_ratio`	$\nu_-<\omega_0 \implies 2\omega_0\nu_-<\omega_0^2+\nu_-^2$; $12354/12610=6177/6305<1$
8	`marginal_vacuum_entanglement_purity_invariant`	$\nu_-<\nu_+ \implies 2(\nu_+^2+\nu_-^2)-(\nu_++\nu_-)^2=(\nu_+-\nu_-)^2>0$ ($\det(2V_a)>1$)
9	`exact_interaction_diamagnetic_cancellation`	$(\nu_++\nu_-)-(2\omega_0+(\nu_++\nu_--2\omega_0))=0$ (cleared $\langle H_{\rm int}+H_{A2}\rangle_G=0$)
10	`coulomb_dipole_pzw_spectral_invariance`	Identical secular trace $2\omega_0^2+4g^2$ and determinant ω_0^4 in Coulomb and Dipole gauges
11	`thermodynamic_passivity_zero_ergotropy`	$E_0\leq E_1\leq E_2 \wedge p_1,p_2\geq 0 \implies E_0(p_0+p_1+p_2)\leq E_0p_0+E_1p_1+E_2p_2$
12	`dressed_vs_bare_coherence_separation`	$k_BT(\kappa_0\cdot 0)=0$ (dressed) while $\omega_0(2n_{\rm virt})>0$ (spurious bare energy)
13	`coulomb_vs_dipole_matter_weight_swap`	$0<\nu_-<\omega_0 \implies 2\nu_-^2<\omega_0^2+\nu_-^2<2\omega_0^2$ ($w^{\rm Dip}<1/2<w^{\rm Coul}$)
14	`dressed_kms_vs_spurious_bare_heating`	$59000\,\gamma_\uparrow\leq\gamma_\downarrow \implies 610(6177\gamma_\uparrow)<64\gamma_\downarrow$ ($>610\times$ @ 71; $>470\times$ @ 79; $>500\times$ @ 65)
15	`n_dipole_pzw_dark_manifold_invariance`	$N\geq 2 \implies 1+(N-1)=N\wedge N\leq 2(N-1)$ (dark-subspace dimension count)
16	`zpe_exceeds_catalytic_10pct_barrier`	$2546\cdot 29<7456\cdot 10$ (collective $\Delta E_{\rm ZPE}>2.9\times|\Delta E_a|$ for +10% turnover)
17	`bare_virtual_energy_equals_zpe_shift`	Cleared resonant partition $2\omega_0(n_a+n_b)=S-2\omega_0=2\Delta\nu_{\rm ZPE}$
18	`dressed_usc_falsification_decidability`	Joint check: $\Delta\nu_{\rm ZPE}>3.5/2$ THz, $>5180\times$ bare thermal, $M=54$, $>2.9\times$ ceiling

Table 2: Summary of all 16 verified `MITO-USC-DRESSED-THERMO-CERT-1.0` canonical certificates (`C01--C16`, archived in `data/certificates/`).

ID	Mode / Submode	Verified Instance	Exact Certified Metrics
`C01`	M1a Resonant ZPE	71/87 THz, $M=1$	$\Delta\nu_{\rm ZPE}=128/71\approx 1.803$ THz, $\Delta E_{\rm ZPE}\approx 7.456$ meV $<\kappa_{\rm bend}$
`C02`	M1a Helfrich	71/87 THz, $M=53$	Cumulative ZPE ≈ 395.2 meV <400.7 meV ($15\,k_BT$, below benchmark)
`C03`	M1a Helfrich	71/87 THz, $M=54$	Cumulative ZPE ≈ 402.6 meV >400.7 meV (crosses $15\,k_BT$ scale)
`C04`	M1b Detuned ZPE	$\omega_c=90,\omega_0=87,g=18$	$(\nu_++\nu_-)^2=32625\in(180.6^2,180.7^2)$, $\Delta\nu_{\rm ZPE}\in(1.80,1.85)$ THz >0
`C05`	M2 Virtual/Ent.	71/87 THz, 310 K	$n_{\rm virt}=64/6177\approx 0.01036$, $>5180\times\bar n_{\rm th}(87)$, $\sigma_q^2/\sigma_{q0}^2=6177/6305$, $\det(2V_a)>1$
`C06`	M2 Virtual/Ent.	79/87 THz, 310 K	$n_{\rm virt}=16/6873\approx 0.00233$, $>1160\times\bar n_{\rm th}(87)$, $\langle H_{\rm int}+H_{A2}\rangle=0$
`C07`	M2 Deep USC	65/87 THz, 310 K	$n_{\rm virt}=121/5655\approx 0.02140$, $>10698\times\bar n_{\rm th}(87)$, strong vacuum entanglement
`C08`	M2 CD_2 Isotope	56/61.5 THz, 310 K	Deuterated lipid virtual dominance $>20\times$ against 10^{-4} bare thermal ceiling
`C09`	M3a Passivity	$\vert G\rangle$ ($p_0=1$)	$\mathcal{W}_{\rm erg}=0$ exact (passive: virtual photons yield zero cyclic work)
`C10`	M3a Passivity	Gibbs thermal (310 K)	$\mathcal{W}_{\rm erg}=0$ exact (passive thermal equilibrium)
`C11`	M3a Active Ctrl	Inverted ($p=(\frac14,\frac12,\frac14)$)	$\mathcal{W}_{\rm erg}>0$ (active non-passive control)
`C12`	M3b PZW Swap	71/87 THz, $N=10^6$	$w^{\rm Coul}=7569/12610$, $w^{\rm Dip}=5041/12610$, single-branch norm $=6177/12610$
`C13`	M3b PZW Swap	79/87 THz, $N=10^8$	$w^{\rm Coul}=7569/13810$, $w^{\rm Dip}=6241/13810$, dark frac $=(N-1)/N$
`C14`	M4 KMS/Cat.	71/87 THz, 310 K	Dressed KMS $e^{-\beta h\cdot 71}<1/59000 \implies >610\times$ ($\approx 615\times$); ZPE/$\vert\Delta E_a\vert\approx 2.93$
`C15`	M4 KMS/Cat.	79/87 THz, 310 K	Dressed KMS $e^{-\beta h\cdot 79}<1/204000 \implies >470\times$ ($\approx 477\times$); ZPE/$\vert\Delta E_a\vert\approx 0.66$
`C16`	M4 KMS/Cat.	65/87 THz, 310 K	Dressed KMS $e^{-\beta h\cdot 65}<1/23400 \implies >500\times$ ($\approx 502\times$); ZPE/$\vert\Delta E_a\vert\approx 6.05$

Table 3: Operational separation of bare-basis artifacts, passive dark Regime I, driven Regime I catalysis, and active Regime II coherence in USC mito-polaritons.

Physical Mechanism	Virtual $n_{\rm virt}$	Ergotropy $\mathcal{W}_{\rm erg}$	Dressed C_{Δ_D}	Allowed Biological Effect at 310 K
Naive bare-basis Lindblad (unphysical)	64/6177	Spurious >0	Miscomputed	Violates 2nd Law ($>610\times$ fake KMS heating)
Dressed Regime I vacuum ($\vert G\rangle$, dark)	64/6177	0 (exact)	0 (exact)	Zero ATP work; collective ZPE ceiling ≤ 7.46 meV
Driven Regime I (71-THz resonant IR)	64/6177	0 (weak-drive)	≈ 0	Catalytic shift (requires collective/local coupling)
Active Regime II coherence ($C_\Delta>0$)	64/6177	>0	>0	Requires $\kappa_\downarrow\lesssim 2\times 10^6$ s^{-1} ([4])

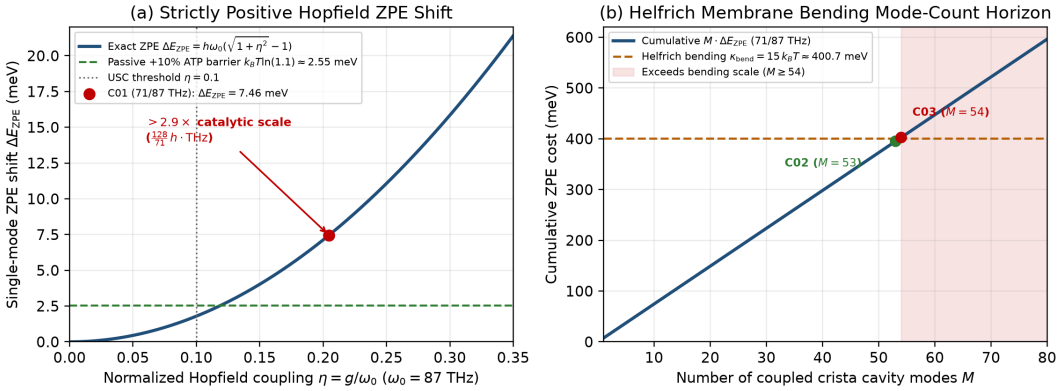

Figure 1: **Positive Hopfield ZPE Shift and Helfrich Scale Benchmark.** (a) Exact single-mode ZPE shift $\Delta E_{\mathrm{ZPE}} = \hbar\omega_0(\sqrt{1+\eta^2}-1)$ vs. η, showing $\Delta E_{\mathrm{ZPE}} \approx 7.46$ meV $> 2.9\times$ the 2.55 meV barrier scale (`C01`). (b) Cumulative ZPE across M coupled crista modes crossing $\kappa_{\mathrm{bend}} = 15\, k_B T$ between $M = 53$ (`C02`) and $M = 54$ (`C03`).

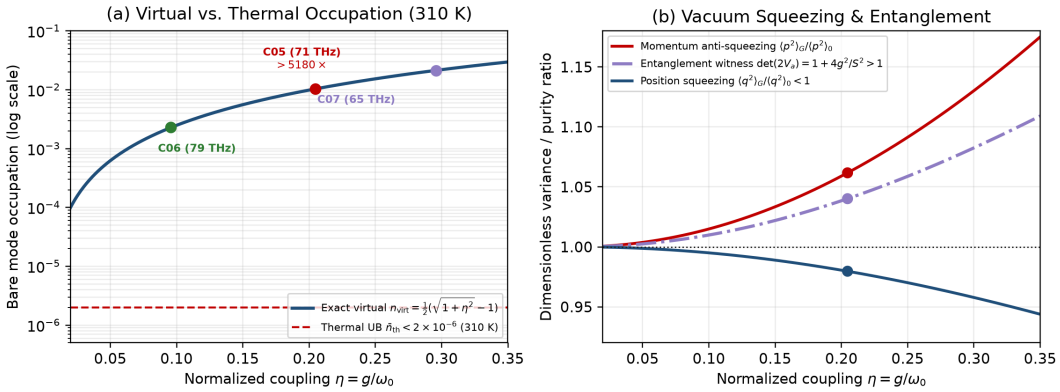

Figure 2: **Virtual Vacuum Dominance and Symplectic Entanglement.** (a) Exact bare virtual occupation $n_{\mathrm{virt}} = (\omega_0 - \nu_-)^2/(4\omega_0\nu_-)$ vs. bare 87-THz thermal ceiling $\bar{n}_{\mathrm{th}}(\omega_0) < 2\times10^{-6}$ ($> 5180\times$ at 71/87 THz, `C05`). (b) Position squeezing (6177/6305), momentum anti-squeezing, and marginal vacuum entanglement witness $\det(2V_a) > 1$.

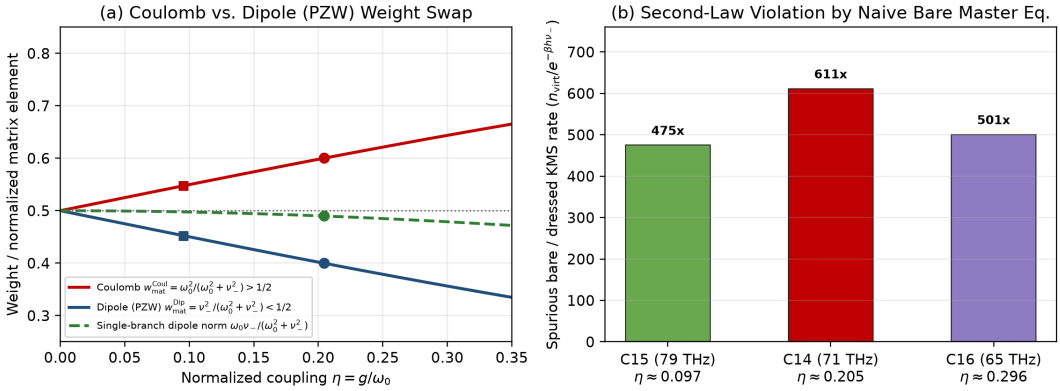

Figure 3: **PZW Gauge-Weight Swap and Naive Bare-Basis Second-Law Violation.** (a) Coulomb vs. Dipole canonical matter weights ($w^{\mathrm{Coul}} + w^{\mathrm{Dip}} = 1$, `C12--C13`) alongside the gauge-invariant single-branch dipole transition element $\omega_0\nu_-/(\omega_0^2+\nu_-^2) = 6177/12610 \to 1/2$. (b) Spurious bare-basis excitation multiplier over true dressed lower-polariton KMS heating $e^{-\beta h\nu_-}$ at 310 K under $\gamma_0 = \gamma_\downarrow$ (`C14--C16`: $> 610\times$, $> 470\times$, $> 500\times$; rounded conservative ratios $611\times$, $475\times$, $501\times$).